Aust. J. Soil Res., 1996, **34**, 623–34

Iron–manganese nodules in a semi-arid environment

A. Sanz[A], *M. T. Garcia-González*[A], *C. Vizcayno*[A], *and R. Rodriguez*[B]

[A] Departmento de Geoquímica y Mineralogía, Centro de Ciencias Medioambientales CSIC Serrano, 115. 28006-Madrid, Spain.
[B] Department de Medi Ambient i Ciencies del Sól, ETSIA. Alcalde Rovira Roure, 144. 25006-Lleida, Spain.

Abstract

Relationships between the chemical, mineralogical, and morphological characteristics and the formation mechanisms of some iron–manganese (Fe–Mn) accumulations were investigated. The nodules studied were from a poorly drained soil profile with a high calcium carbonate content, located in a semi-arid environment.

Three types of nodules, Fe-rich (typic or annular morphology), Mn-rich (aggregate morphology), and Fe–Mn-rich (compound morphology), were encountered, all of which were formed *in situ*.

The nodules were found to contain goethite, and a low proportion of poorly crystallised Fe oxides and Mn oxides (birnessite and vernadite). However, they contained no siderite or rhodochrosite, both highly frequent occurrences in carbonatic systems with redox fluctuations.

In the formation of compound nodules, Fe- and Mn-rich nodules may act as nucleating structures for subsequent accumulations in the form of coatings and/or matrix impregnations.

Additional keywords: Fe–Mn, morphology, birnessite, goethite.

Introduction

Iron and/or manganese accumulations in natural systems have often been explained in terms of variations in both the oxidation–reduction potential (pe) and hydrogen ion activity (pH) (Collins and Buol 1970; Skinner and Fitzpatrick 1992), the presence of other ions commonly found in the environment such as CO_3^{2-} (Mania *et al.* 1989; Matsunaga *et al.* 1993), and microbiological action (Chukhrov *et al.* 1980; Golden *et al.* 1992).

We studied the relationships between the chemical, mineralogical, and morphological characteristics of various Fe–Mn accumulations, and their formation mechanisms. The nodules were from a poorly drained soil with a high calcium carbonate content located in a semi-arid environment.

Materials and methods

The soil profile studied is located in the Flumen–Monegros irrigation district, in the province of Huesca (north-eastern Spain). The materials of the area are Tertiary saline mudstone and sandstone, covered mostly by Quaternary deposits. The climate is semi-arid Mediterranean, with mean annual rainfall, temperature, and evapotranspiration (ET_O, Blaney–Criddle method) of 480 mm, 14·5°C, and 1200 mm, respectively.

The profile lies in a poorly drained endorheic depression and its parent material consists of fine detritic Holocene sediments with high calcium carbonate content and salinity–sodicity level. In 2 observations, the watertable depth was found to be 180 and 280 cm. The profile is currently drained and flood-irrigated. Its macromorphological and chemical characteristics

0004-9573/96/050623$05.00

Table 1. Major macromorphological features of the soil profile

Texture: C–L, clay loam; S-C, silty clay; C, clay. Form: sb, subangular; pr, prismatic. Size: m, medium. Grade: w, weak; m, medium; s, strong; vs, very strong. Ox, oxidation; red, reduction; fw, few; fr, frequent; c, common; h, hard; fb, friable

Horizon	Depth (cm)	Colour (moist)	Textural class USDA	Structure (form, size, grade)	Mottles	Coatings	Carbonatic nodules	Fe–Mn nodules
Ap1	0–15	10 YR 4/6	C–L	sb, m, w	ox, fw	–	–	–
Ap2g	15–34	10 YR 4/6	C–L	sb, m, w	ox, fw; red, fr	–	–	–
Bwg	34–65	10 YR 6/6	S–C	sb, m, m	red, fr	–	fw, h	fw, 7·5 YR 3/2
Bkncg1	65–98	10 YR 5/7	S–C	1*a* pr, m, m 2*a* sb, m, s	red, fr	fr	fr, h	fr, 7·5 YR 3/2
Bkncg2	98–130	10 YR 5/6	C	1*a* pr, m, m 2*a* sb, m, s	ox, fr; red, fw	fr	c, h	fw, 7·5 YR 3/3
2Bkng	130–175	7·5 YR 5/6	C	1*a* pr, m, vs 2*a* sb, m, s	ox, fr	c	c, fb	fw, 7·5 YR 3/3

Table 2. Chemical characteristics of the soil profile

Horizon	Organic matter (%)	$CaCO_3$ equiv. (%)	pH (paste)	EC (dS/m)	Soluble ions (cmol/L) Ca^{2+}	Mg^{2+}	Na^{+}	Cl^{-}	SO_4^{2-}	CO_3^{2-}	HCO_3^{-}	SAR
Ap1	1·23	18·46	8·1	4·60	1·00	1·09	2·79	2·54	1·37	n.d.	0·75	8·6
Ap2g	1·08	13·77	8·1	10·00	1·80	1·22	7·46	7·03	2·65	n.d.	0·58	19·2
Bwg	1·08	16·93	8·2	11·50	1·61	0·80	9·49	8·20	2·85	n.d.	0·48	27·3
Bkncg1	0·95	16·16	8·4	12·41	2·41	1·51	10·08	9·16	3·80	n.d.	0·33	21·1
Bkncg2	0·75	15·17	8·3	10·36	1·52	1·09	8·60	6·94	3·43	n.d.	0·36	23·8
2Bkng	0·43	17·09	8·3	9·63	1·35	1·38	8·41	7·15	3·04	n.d.	0·40	22·7

n.d., not detected.

are summarised in Tables 1 and 2. The soil was classified as Aquic Xerochrept, fine, mixed (calcareous), thermic (Soil Survey Staff 1992).

Micromorphological characteristics were determined by using air-dried undisturbed blocks of the horizons that were impregnated with polystyrene resin. Thin sections were described according to Bullock *et al.* (1985).

Submicromorphological studies were made by using a Zeiss DSM 940A scanning electron microscope (SEM) equipped with a back-scattered electron detector (BSE) and an Oxford Link 5118 energy dispersive X-ray spectrometer (EDS). The thin sections previously prepared for the micromorphological study, and selected nodules, were used for examinations. Some nodules were embedded in LR White resin and cross-cut, whereas others were fractured and observed directly. All samples were coated with carbon prior to examination.

Mineralogical identification was performed with a Philips X'Pert diffractometer (graphite monochromated CuKα radiation) and random powder patterns. In order to separate the XRD contributions of the different mineralogical species, a Cauchy distribution function was used to fit the diffraction patterns.

Hydroxylamine hydrochloride (hahc, Chao 1972) was used to extract Mn oxide minerals at pH 3·6 in order to avoid dissolving iron oxides. Oxalate (ox, Schwertmann 1964) and dithionite-citrate-bicarbonate (dcb, Mehra and Jackson 1960) were used to extract poorly ordered Fe oxides and crystalline Mn and Fe oxides, respectively. Elemental quantitative analyses were carried out by ICP spectroscopy (Perkin-Elmer 5500). Mn oxides were concentrated by flotation with H_2O_2 (Taylor *et al.* 1964).

Table 3. Micromorphological characteristics of the Fe–Mn accumulations

br, brown; or, orange; r, red; rb, reddish brown; di, diffuse; cl, clear; sh, sharp; pr, present

Accumulation type and internal morphology	Impregnation	Proportion (%)	Size (μm)	Colour	External morphol./limit
		Bwg			
Mottles	Weak	2	20–100	br	Dendrite/di
Hypo-coatings	Weak	1	15–30	br	—
Nodules					
Typic	Very weak	1	50–200	or–r	Round/cl
Concentric	Moderate	1	50–200	or–r	Round/cl
Compound	Moderate	pr	100–1000	br–rb	Round/sh
		Bkncg1			
Mottles	Weak	1	20–100	br	Dendrite/di
Hypo-coatings	Weak	pr	15–30	br–rb	—
Nodules					
Aggregate	Weak	pr	50–300	br	Subround/sh
Typic	Weak	1	50–300	or–r	Round/cl
Annular	Weak	1	50–300	or–r	Round/cl
Compound	Moderate	6	100–2000	br–rb	Round/cl
		Bkncg2			
Mottles	Weak	1	20–200	br	Dendrite/di
Nodules					
Aggregate	Weak	pr	50–250	br	Subround/sh
Typic	Weak	pr	50–300	r–or	Round/cl
Compound	Weak	pr	100–2000	br–rb	Round/cl
		2Bkng			
Mottles	Very weak	1	15–200	br	Dendrite/di
Hypo-coatings	Very weak	pr	—	—	—
Quasi-coatings	Very weak	pr	—	—	—

Chemical and XRD analyses were made by using several fractions of the soil horizons ($\leq$2 mm, 50–8 μm, 8–2 μm, and $\leq$2 μm) and selected nodules obtained by wet sieving (2–1, 1–0·63, 0·63–0·4, and 0·4–0·25 mm) of the Bkncg1 horizon.

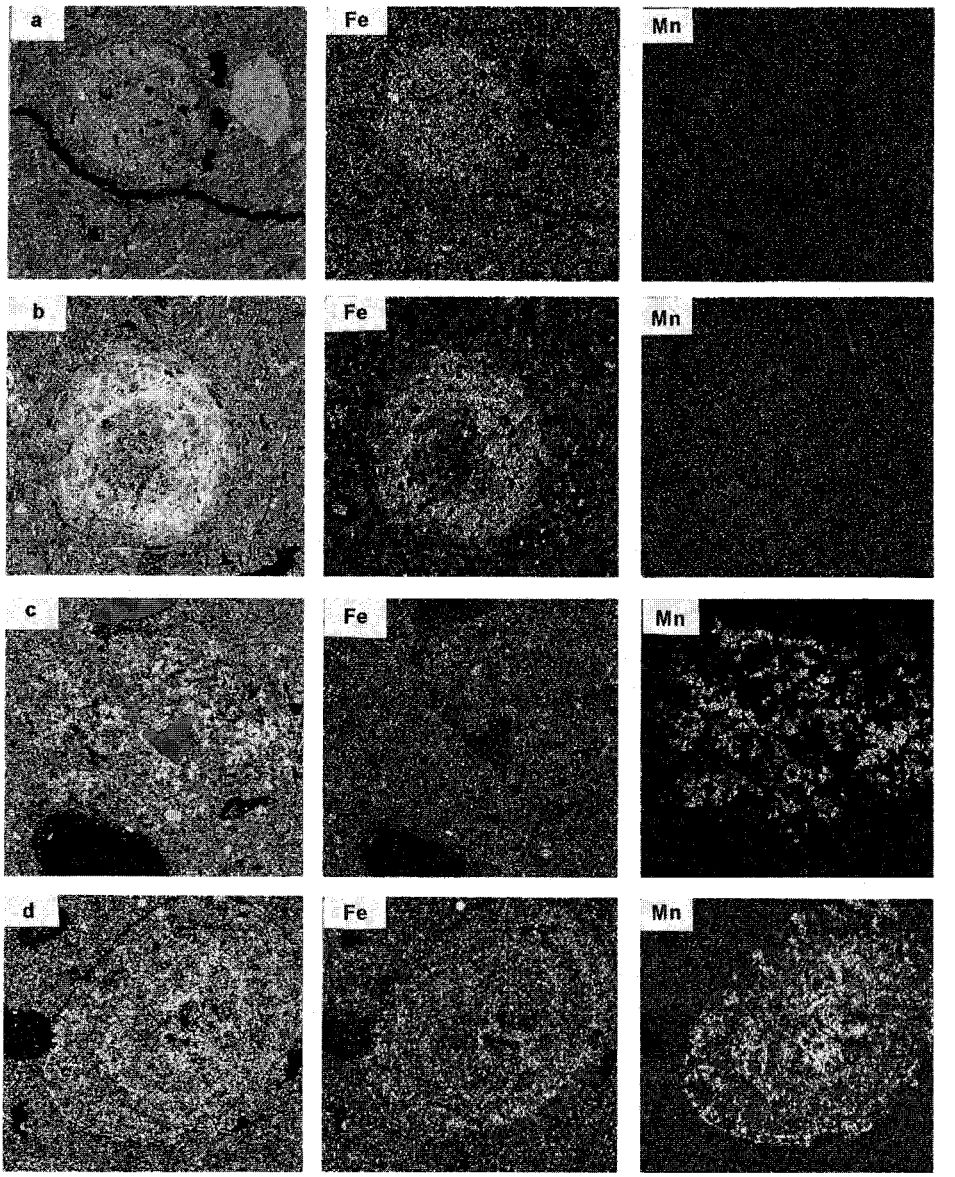

Fig. 1. Back-scattered electron (BSE) images and X-ray distribution images of Mn and Fe in different types of nodules (thin section of Bkncg1 horizon): (*a*) typic, (*b*) annular, (*c*) aggregate, (*d*) compound. The width across each image is (*a*) 300 μm, (*b*) and (*c*) 350 μm, (*d*) 1350 μm.

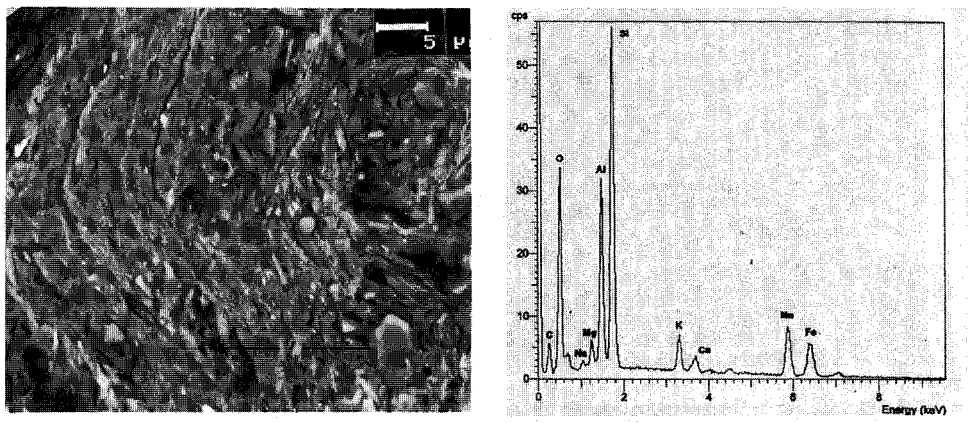

Fig. 2. BSE image and EDS X-ray spectrum of some cumulative stages in a compound nodule.

Results

Morphological study

Light microscopy

Thin section analyses of the soil horizons revealed the presence of mottles, coatings, and nodules of Fe–Mn in the B horizons (Table 3). The nodules were found to be of various types with variable internal morphology: typic, annular, aggregate, and compound (the last being a mixture of the previous three). Nodule concentration and size were maximal in the Bkncg1 horizon, where the compound morphology was the most frequent. Nodules and mottles exhibited an unreferred distribution in the soil matrix.

Scanning electron microscopy

The SEM study of the thin sections revealed 2 types of Fe-rich nodules with a uniform and annular Fe distribution (Fig. 1*a*, *b*). Mn-rich nodules exhibited a dendritic aggregate structure where little or no Fe was present (Fig. 1*c*). Finally, compound nodules showed a concentric pattern formed by Fe and/or Mn cumulative stages (Figs 1*d*, 2).

Curved planar voids in the nodules were coated with convoluted and parallel bands (Fig. 3*a*), while vugh voids exhibited signs of microbiological activity (Fig. 3*b*). Mn bands were thicker than Fe bands and porous to a variable degree (Fig. 3*c*, *e*). Two types of coating compositions were observed; thus, Fe-rich nodules only contained a small amount of Mn (Fig. 4), whereas Mn-rich nodules contained Ba, Ca, and a low proportion of Fe (Fig. 5).

Chemical study

The major part of the little Mn_{dcb} extracted from the soil horizons (Fig. 6) was from the Bwg and Bkncg1 horizons. The low Fe_{ox}/Fe_{dcb} ratio obtained (Fig. 6) revealed Fe to be mostly crystalline and the Ap1 and Bkncg1 horizons to contain the greatest concentrations of poorly crystallised Fe.

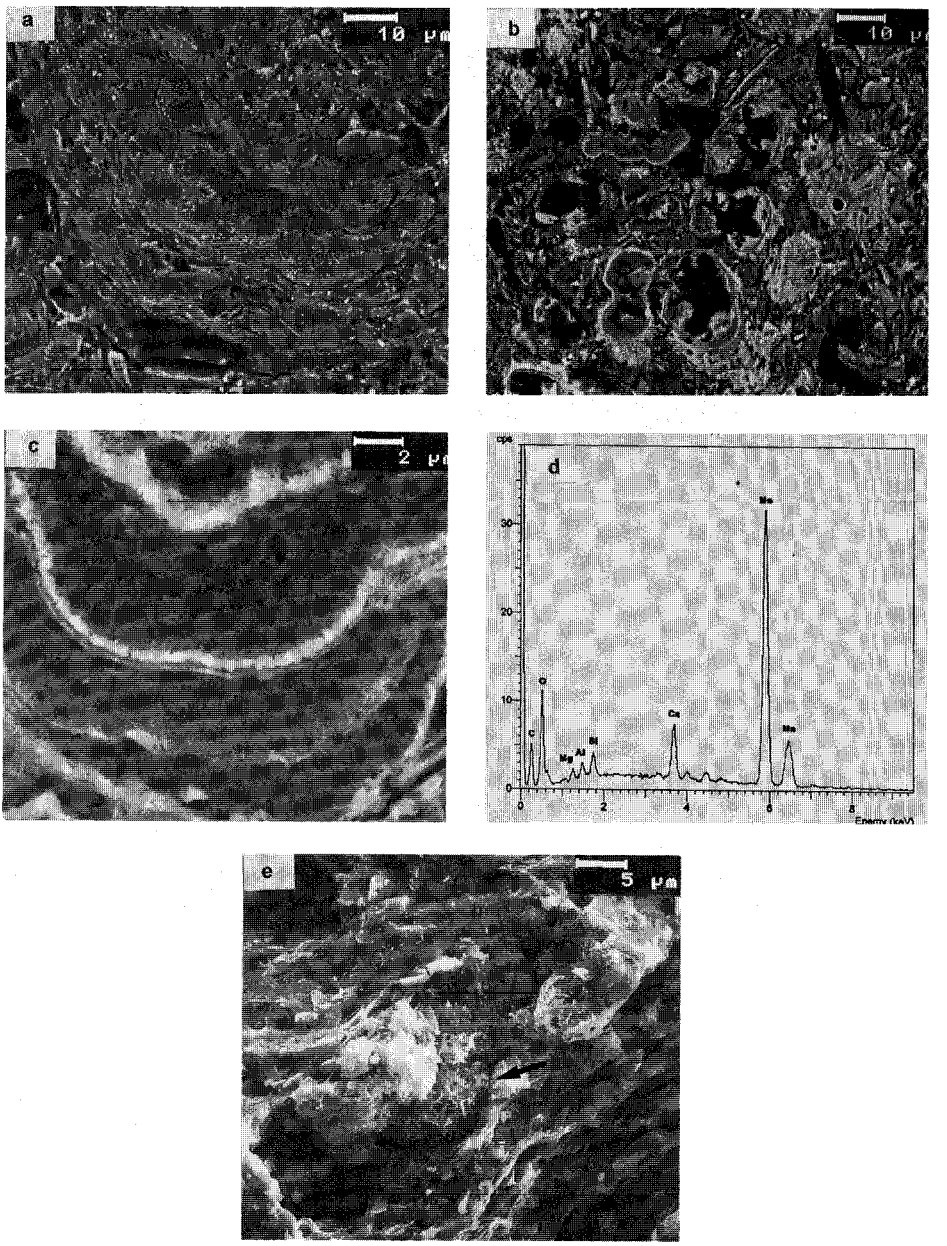

Fig. 3. Compound nodule: (*a*) BSE image of a coating with convoluted bands in a curved planar void, (*b*) BSE image of coatings in vugh voids, (*c*) BSE image and (*d*) EDS X-ray spectrum of a Mn accumulation of variable porosity, (*e*) SE image showing a fluffy Mn aggregate.

Mn extraction from all nodule fractions was maximal for dcb and much lower for hahc and ox (Fig. 7*a*). According to Schwertmann and Fanning (1976), the Mn concentration decreases with decreasing nodule size, irrespective of the extractant used. The fact that the amount of Mn extracted by dcb was much

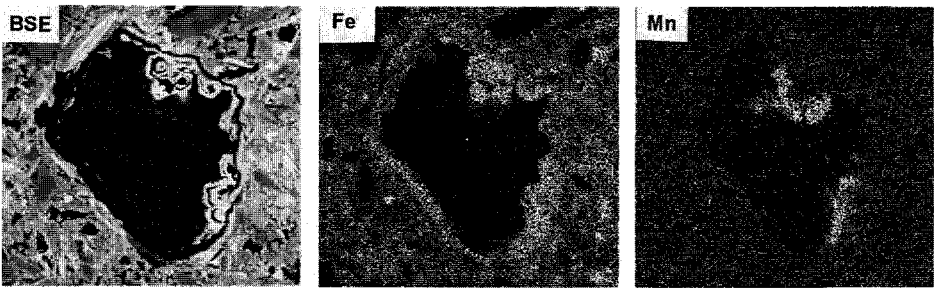

Fig. 4. BSE and X-ray distribution images of a Fe-rich coating. The width across each image is 90 μm.

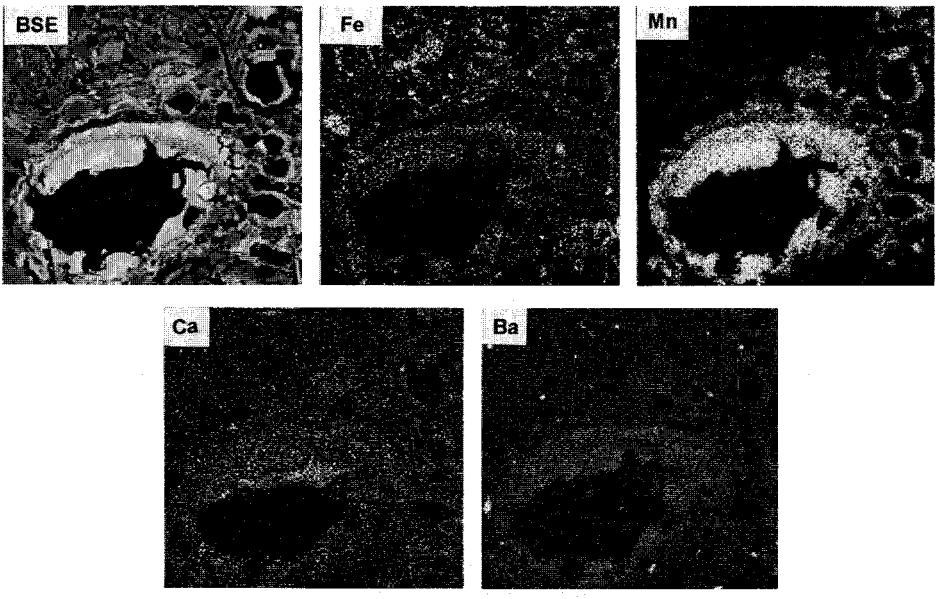

Fig. 5. BSE and X-ray distribution images of a Mn-rich coating. The width across each image is 90 μm.

greater than that extracted by hahc and ox may have been the result of a close association between crystalline-Fe and Mn in the nodules (Jarvis 1984).

There was no correlation between the amount of Fe extracted by dcb and nodule size (Fig. 8); it is remarkable that dcb extracted a large amount of Fe. Fe extraction by hahc was very low (Fig. 8), but increased with nodule size. These results suggest a close association between Fe and Mn extracted by hahc.

The fact that the amount of Fe extracted by hahc is extremely low (Fig. 8) leads us to associate Mn_{hahc} with the extracted heavy metals Co, Ni, and Zn. This is further supported by a positive correlation between Ni–Mn and Co–Mn (Fig. 7*b*), also consistent with previous results of Burns (1976). Mn and Zn contents were not well correlated.

Mineralogical study

XRD results for the different size fractions from the soil horizons revealed quartz and calcite to be the major components of the coarse fractions. In the 8–2 μm

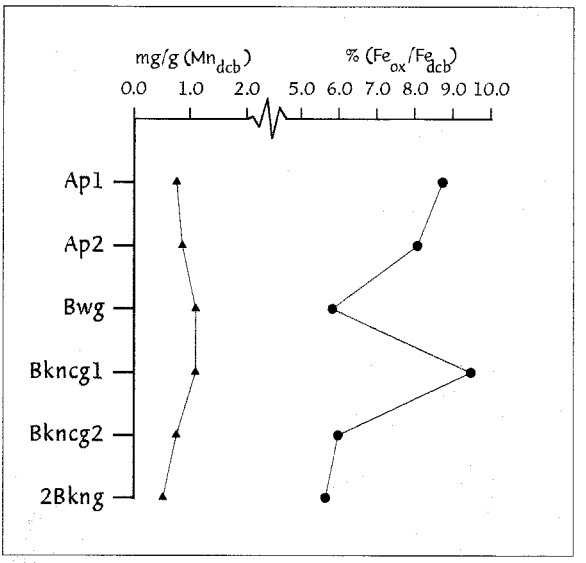

Fig. 6. Mn_{dcb} concentration and Fe_{ox}/Fe_{dcb} ratio in the soil profile.

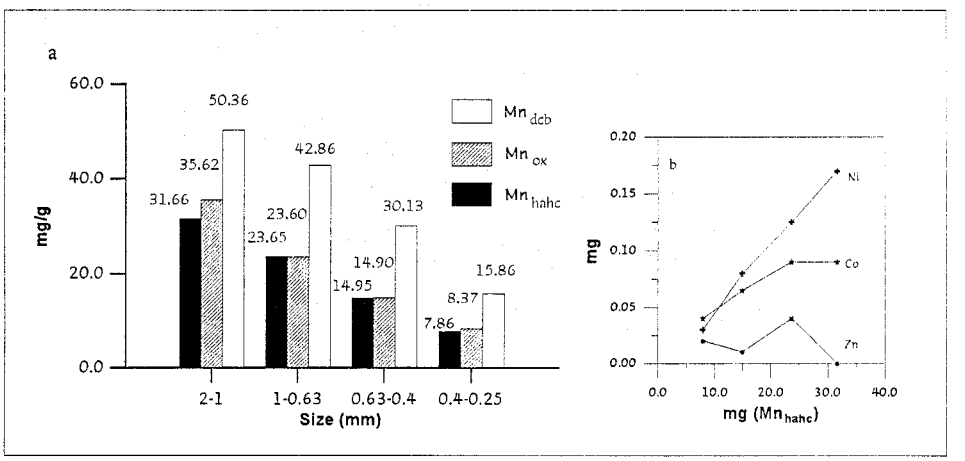

Fig. 7. (*a*) Concentration of Mn extracted by hydroxylamine (hahc), oxalate (ox), and dithionite (dcb) from selected nodules. (*b*) Relationship between Ni, Co, Zn, and Mn extracted by hydroxylamine (hahc) from the same selected nodules.

fraction, illite, quartz, and calcite were present in similar proportions, illite being the main mineral in the clay fraction (≤ 2 μm). Chlorite and pyrophyllite were also present in the fine fractions (≤ 8 μm), while goethite was only encountered in the clay fraction.

The mineralogy of the different nodule sizes was similar. Quartz was the main phase, and small amounts of dioctahedral mica, chlorite, goethite, feldspars, and calcite were also present (see Fig. 10). No Mn minerals could be identified.

The curve-fitted XRD pattern for the H_2O_2 flotation sample (region 11–14° 2θ, Fig. 9) revealed the presence of birnessite (broad reflection about 0·720 nm) and chlorite (peak at 0·707 nm). In the region 36–38° 2θ (Fig. 10), the hahc treatment showed the loss of calcite (peak at 0·250 nm) and a decrease in band

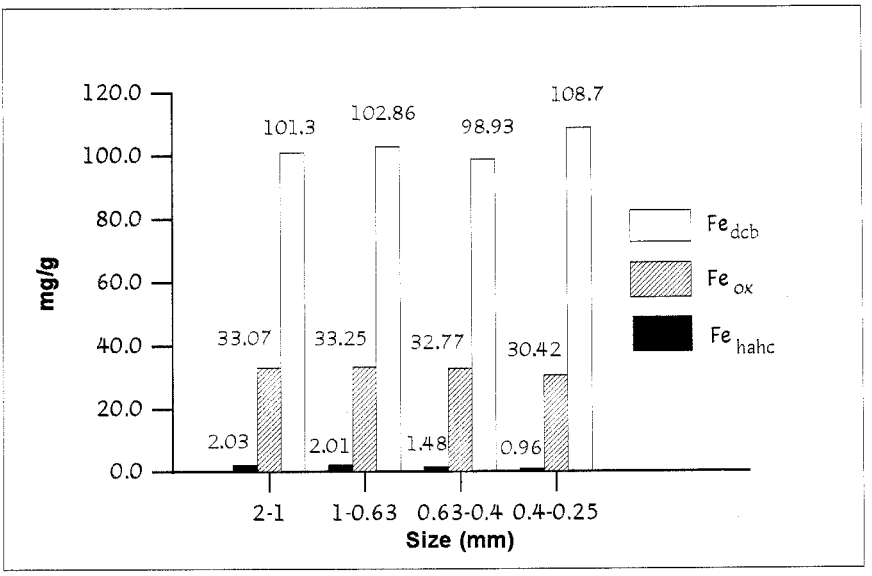

Fig. 8. Concentration of Fe extracted by hydroxylamine (hahc), oxalate (ox), and dithionite (dcb) from selected nodules.

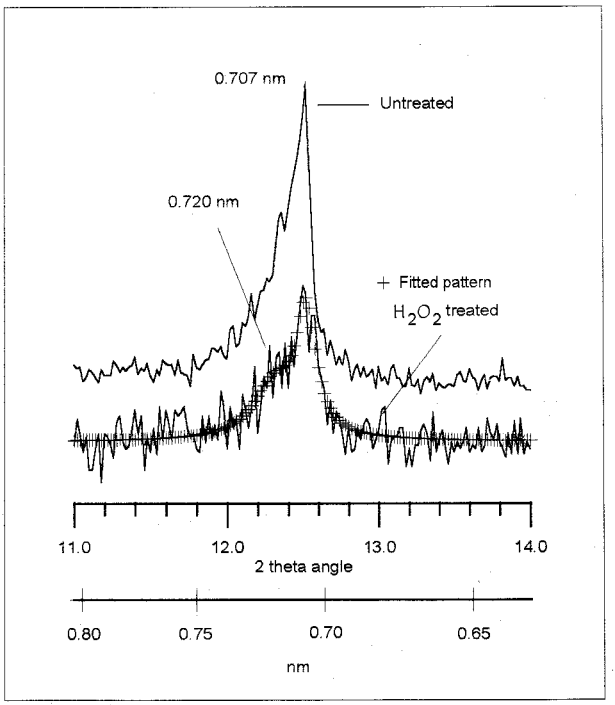

Fig. 9. Diffraction patterns of selected nodules (1–0·63 mm).

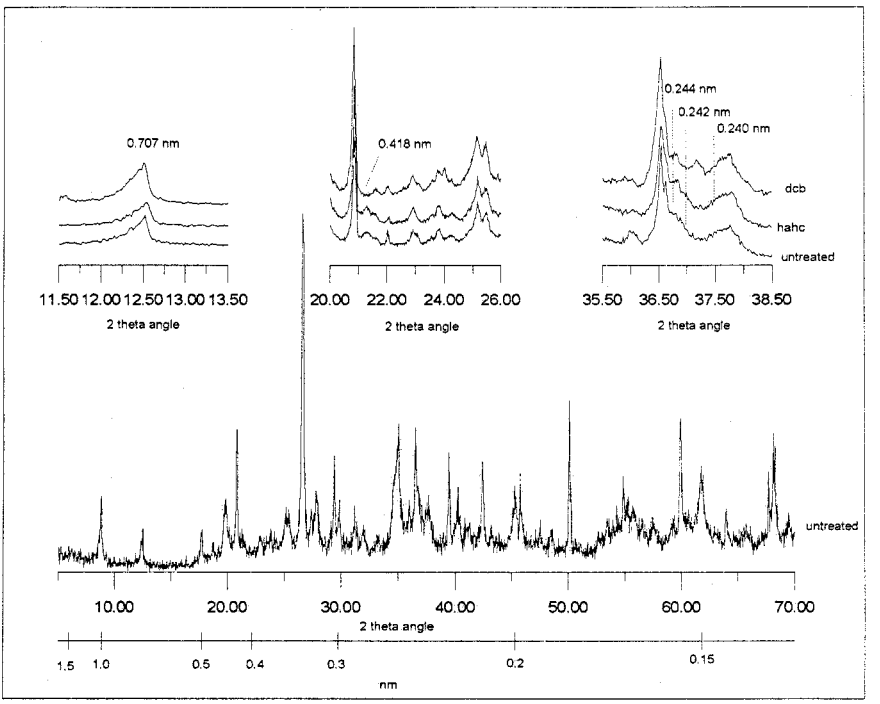

Fig. 10. Diffraction patterns of selected nodules (2–1 mm).

intensity in the range 0·244–0·242 nm. The dcb treatment (on the sample previously ox treated) revealed the loss of effects such as those at 0·244 (goethite), 0·242 (birnessite), and 0·240 nm (vernadite). Feldspars were also identified from a peak at 0·241 nm.

Discussion

The results suggest that the nodules were formed *in situ*. The largest nodules were reddish brown in colour, of compound morphology, and Fe- and Mn-rich regarding chemical composition. Smaller nodules were brown (of aggregate morphology and Mn-rich) or rusty (of typic and annular morphology and Fe-rich). According to Richardson and Hole (1979) and Veneman and Bodine (1982), Fe and Mn redistribution in soil is caused by water table oscillations; for this reason, the Bkncg1 horizon had the highest concentration of compound nodules. On the other hand, capillary uprise of Mn as Mn^{2+} (Pickering and Veneman 1984) led to the formation of mottles and coatings of Mn, small Fe nodules, and a low proportion of compound nodules in the Bwg horizon.

The micromorphological study revealed the nodules of size 2 to 0·25 mm to have a compound morphology; the other types of morphology were encountered in nodule sizes below 300 μm. Thus, the decrease in the Mn_{hahc}/Mn_{dcb} ratio with decreasing nodule size could be the result of a stronger interlayer association between Mn and Fe in the smaller nodules. This tendency was broken in the nodules of size 0·40–0·25 mm owing to the presence of pure Fe nodules, which is supported by the increased amount of Fe extracted by dcb. According to

McKenzie (1989), the occurrence of an essentially interlayer association between Fe and Mn is characteristic of the presence of incipient nodules; as a result, the nodules in the size range 0·63–0·40 mm must be those containing the highest concentrations of incipient nodules.

So far, siderite and rhodochrosite have been the Fe- and Mn-bearing minerals formed in carbonatic systems under alternating redox conditions (Mania *et al.* 1989; Matsunaga *et al.* 1993). However, in this work we detected goethite and poorly crystallised Mn oxides (birnessite and vernadite) as the likely result of other factors such as microbiological activity (Golden *et al.* 1992), the action of mixed Fe and Mn oxides as nucleants for manganic phases (McKenzie 1989), and Mn auto-oxidation (Sullivan and Koppi 1992).

The formation mechanism for the compound nodules may involve typic and annular Fe nodules, and aggregate Mn nodules, as nucleating structures for subsequent accumulations. These may be deposited in pores or in the soil matrix. The former would lead to more or less complex Fe and/or Mn coatings; the latter would give rise to cementation processes producing fissures that may subsequently be filled up or lead to a new individual nodule with a more complex morphology than the original one.

Conclusions

Three types of nodules, rusty (Fe-rich, of typic or annular morphology), brown (Mn-rich, of aggregate morphology), and reddish brown (Fe- and Mn-rich, of compound morphology) were found. All these accumulations were formed *in situ*, in a carbonatic, poorly drained system located in a semi-arid environment.

Because of the essentially interlayer association between Fe and Mn, the nodules of size 0·63–0·40 mm contained the highest concentrations of incipient compound nodules.

As mineralogical phases of Fe and Mn, the nodules contain goethite, and a low proportion of poorly crystallised Fe oxides and Mn oxides (birnessite and vernadite). It is worth noting the lack of siderite and rhodochrosite, 2 frequently occurring minerals in carbonatic systems under redox fluctuations.

In the formation of compound nodules, Fe- and Mn-rich nodules may act as nucleating structures for subsequent accumulations in the form of coatings and/or matrix impregnations.

Acknowledgments

The authors are grateful to Dr Wierzchos for his help in relation to the SEM study, and to Mrs Lázaro for technical assistance. This research was supported by DIGICYT (Spain), Project PB 90/90.

References

Bullock, P., Fedoroff, N., Jongerius, A., Stoops, G., and Tursina, T. (1985). 'Handbook for Soil Thin Section Description.' (Waine Research Publications: Wolverhampton, UK.)

Burns, R. G. (1976). The uptake of cobalt into ferromanganese nodules, soils and synthetic manganese (IV) oxides. *Geochimica et Cosmochimica Acta* **40**, 95–102.

Chao, T. T. (1972). Selective dissolution of manganese oxides from soils and sediments with acidified hydroxylamine hydrochloride. *Soil Science Society of America Proceedings* **36**, 764–8.

Chukhrov, F. V., Gorshkov, A. I., Rudnitskaya, E. S., Beresovskaya, V. V., and Sivtsov, A. V. (1980). Manganese minerals in clays: a review. *Clays and Clay Minerals* **28** (5), 346–54.

Collins, J. F., and Buol, S. W. (1970). Effects of fluctuations in the Eh-pH environment on iron and/or manganese equilibria. *Soil Science* **110** (2), 111–18.

Golden, D. C., Zuberer, D. A., and Dixon, J. B. (1992). Manganese oxides produced by fungal oxidation of manganese from siderite and rhodochrosite. *Catena Supplement* **21**, 161–8.

Jarvis, S. C. (1984). The forms of occurrence of manganese in some acidic soils. *Journal of Soil Science* **35**, 421–9.

Mania, J., Chauve, P., Remy, F., and Verjus, P.(1989). Evolution of iron and manganese concentrations in presence of carbonates and clays in the alluvial groundwaters of the Ognon (Franche-Comté, France). *Geoderma* **44**, 219–27.

Matsunaga, T., Karametaxas, G., Gunten, H. R. von, and Lichtner, P. C. (1993). Redox chemistry of iron and manganese minerals in river-recharged aquifers: a model interpretation of a column experiment. *Geochimica et Cosmochimica Acta* **57**, 1691–704.

McKenzie, R. M. (1989). Manganese oxides and hydroxides. *In* 'Minerals in Soil Enviroments'. (Eds J. B. Dixon and S. B. Weed.) pp. 439–65. (Soil Science Society of America: Madison, WI.)

Mehra, O. P., and Jackson, M. L. (1960). Iron oxide removal from soils and clays by a dithionite-citrate system buffered with sodium bicarbonate. Proceedings 7th National Conference. *Clays and Clay Minerals* **9**, 317–27.

Pickering, E. W., and Veneman, P. L. M. (1984). Moisture regimes and morphological characteristics in a hydrosequence in central Massachusetts. *Soil Science Society of America Journal* **48**, 113–18.

Richardson, J. L., and Hole, F. D. (1979). Motting and iron distribution in a Glossoboralf-Haplaquoll hydrosequence on a glacial moraine in northwestern Wisconsin. *Soil Science Society of America Journal* **43**, 552–8.

Schwertmann, U. (1964). The differentiation of iron oxides in soils by a photochemical extraction with acid ammonium oxalate. *Zeitschrift Pflanzenernährung Dueng Bodenkunde* **105**, 194–202.

Schwertmann, U., and Fanning, D. S. (1976). Iron–manganese concretions in hydrosequences of soils in loess in Bavaria. *Soil Science Society of America Journal* **40**, 731–8.

Skinner, H. C. W., and Fitzpatrick, R. W. (1992). Iron and manganese biomineralization. *Catena Supplemant* **21**, 1–6.

Soil Survey Staff (1992). 'Keys to Soil Taxonomy.' 15th Edn. SMSS Technical Monograph 19. (Pocahonias Press: Backsburg, VA.)

Sullivan, L. A., and Koppi, A. J. (1992). Manganese oxide accumulations associated with some soil structural pores. I. Morphology, composition and genesis. *Australian Journal of Soil Research* **30**, 409–27.

Taylor, R. M., McKenzie, R. M., and Norrish, K. (1964). The mineralogy and chemistry of manganese in some Australian soils. *Australian Journal of Soil Research* **2**, 235–48.

Veneman, P. L. M., and Bodine, S. M. (1982). Chemical and morphological characteristics in a New England drainage-toposequence. *Soil Science Society of America Journal* **46**, 359–63.

Manuscript received 18 December 1995, accepted 14 May 1996